CANCRINITE-GROUP MINERALS AT NON-AMBIENT CONDITIONS: A MODEL OF THE ELASTIC BEHAVIOR AND STRUCTURE EVOLUTION

PAOLO LOTTI

Dipartimento di Scienze della Terra, Università di Milano, Via Botticelli 23, 20133 Milano

INTRODUCTION

More than ten mineralogical species and a large number of synthetic compounds belong to the cancrinite group (Bonaccorsi & Merlino, 2005; Pekov *et al.*, 2011). All of them share the [CAN] framework type (Baerlocher *et al.*, 2007), which is part of the so-called ABC-6 family. This framework is made by columns of base-sharing "*can*" units (or cancrinite cages, undecahedral cages), surrounding iso-oriented large channels bound by twelve-membered rings of tetrahedra (12R-channel; Fig. 1). The [CAN]-framework can also be described as built by double *zigzag* chains (*dzc* unit, Baerlocher *et al.*, 2007), running along [0001] and made by edge-sharing four-membered rings of tetrahedra (S4R) (Fig. 1). The cage voids are linked to the channel systems through narrow six-membered ring windows (S6R∠[0001]) (Fig. 1).
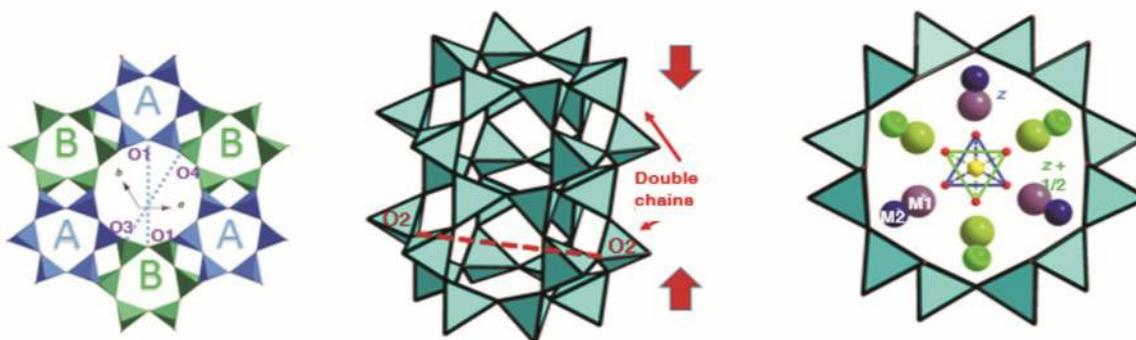

Fig. 1 - a) The [CAN]-type framework viewed down [0001]. «A-» and «B-type» positions of the 6-membered rings (corresponding to the cage basis) are shown, along with the channel diameters O1-O1 and O3-O4. b) A column of cages, where the O2-O2 diameter within the (0001) plane and the double chains of tetrahedra are marked. c) The channel extraframework population in davyne viewed down [0001]. The «internal» M1 site is occupied by K^+, while the «external» M2 by Na^+. The S atom and the oxygen atoms belonging to the SO_4^{2-} bases are shown in yellow and red, respectively.

With the only exception of tiptopite, the minerals of the cancrinite group all show an aluminosilicate framework. They can be found in alkali-rich and SiO_2-undersaturated rocks, generally formed during the effusive and late intrusive stages of alkaline magmatism and related contact metamorphism (*e.g.*, Deer *et al.*, 2004; Bonaccorsi & Merlino, 2005; Pekov *et al.*, 2011). The cancrinite group minerals can be classified into two subgroups according to the extraframework content. In the "cancrinite subgroup", the columns of cages are filled by chains of $[Na-H_2O]^+$ clusters, whereas in the "davyne subgroup" the cages are filled by $[Ca-Cl]^+$ clusters. The center of the channel is filled by several types of anionic and molecular groups (*e.g.*, CO_3^{2-}, SO_4^{2-}, Cl^-, PO_4^{3-}, and $C_2O_4^{2-}$; Bonaccorsi & Merlino, 2005; Pekov *et al.*, 2011, and references therein). The Na^+ cations, partially replaced by K^+ and/or Ca^{2+} (see Pekov *et al.*, 2011, for crystal chemical considerations), fill the positions close to the channel wall (Fig. 1). An even larger chemical variability is shown by the synthetic cancrinites reported in the literature, regarding not only the extraframework population, but also the framework composition. The cancrinite-group compounds can be readily found in several processes of environmental and/or economic concern; of particular interest is the large precipitation of (NO_3^-)-cancrinites from Na-rich caustic nuclear waste

solutions at the Hanford site (Washington, USA) showing an incorporation capacity for Cs^+ ions into the structural cages (Zhao *et al.*, 2004), arising the interest on these compounds as storage materials for alkaline waste solutions (*e.g.*, Bao *et al.*, 2005).

AIM OF THE PROJECT AND EXPERIMENTAL METHODS

The knowledge of the phase-stability fields and the description of the thermo-elastic behavior of the cancrinite-group minerals play a key role in the characterization of the natural and industrial processes in which these compounds are primary constituents. The aim of this study is to provide a model of 1) the thermo-elastic behavior, 2) the (*P*, *T*)-induced structure evolution, at the atomic scale, of the minerals belonging to this group, and, in particular, 3) the influence played by the different extraframework constituents on the structure deformation mechanisms at non-ambient conditions.

The study at high pressure, low and high temperature, by *in-situ* single-crystal X-ray diffraction, was restricted to the most common minerals of the group, *i.e.*, (CO_3)-rich and (SO_4)-rich end-members of the two aforementioned subgroups: cancrinite *sensu stricto* $\{[(Na,Ca)_6(CO_3)_{1.2-1.7}][Na_2(H_2O)_2][Al_6Si_6O_{24}]\}$ and vishnevite $\{[(Na,Ca,K)_6(SO_4)][Na_2(H_2O)_2][Al_6Si_6O_{24}]\}$, balliranoite $\{[(Na,Ca)_6(CO_3)_{1.2-1.7}][Ca_2Cl_2][Al_6Si_6O_{24}]\}$ and davyne $\{[(Na,Ca,K)_6((SO_4),Cl_2)][Ca_2Cl_2][Al_6Si_6O_{24}]\}$, respectively. The natural samples used in this study all showed chemical compositions consistent to those of the end-members reported above. The crystals of cancrinite $[Na_{6.59}Ca_{0.93}[Si_{6.00}Al_{6.00}O_{24}](CO_3)_{1.04}F_{0.41}\cdot 2H_2O]$ were cut from a gem-quality sample from Cava Satom (Cameroon). The gem-quality balliranoite sample $[(Na_{4.47}Ca_{2.86}K_{0.11})(Si_{5.96}Al_{6.04}O_{24})Cl_{2.03}(CO_3)_{0.78}(SO_4)_{0.33}]$ is from Dattaw (Mogok Metamorphic Belt, Myanmar), where crystallized in a skarn-like environment by the interaction of granite and its fluids with the marble wallrocks and corundum inclusions. The davyne sample $[(Na_{3.72}K_{1.86}Ca_{1.97}Sr_{0.04}Mg_{0.02}Ba_{0.01})(Si_{5.93}Al_{6.07}O_{24})(SO_4)_{0.51}Cl_{2.00}]$ was found in a cavity of a skarn lithic block within volcanic deposits at Monte Somma (Naples, Italy). The vishnevite sample $[(Na_{5.22}K_{1.64}Ca_{0.07}Sr_{0.01})(Si_{6.13}Al_{5.87}O_{24})(SO_4)_{0.58}]$ is from the type locality, Vishnevye Gory (Urals, Russia). The high-pressure behavior of cancrinite (Lotti *et al.*, 2012) and balliranoite (Lotti *et al.*, 2014a) was investigated up to 6.63(2) and 6.77(2) GPa, respectively, using a KUMA KM4 point-detector (for unit-cell parameters measurement) and an Oxford Diffraction Xcalibur CCD (for structure analysis) single-crystal diffractometers (both with Mo-*K*α radiation). The high-pressure experiments on davyne (Lotti *et al.*, 2014b) and vishnevite were performed, up to 7.18(6) and 7.40(4) GPa, respectively, at the ID09A beamline (λ = 0.414 Å) of the European Synchrotron Radiation Facility (ESRF, Grenoble, France). For all the experiments, hydrostatic high-pressure conditions on the studied samples were generated by diamond anvil cells, using a 4:1 methanol:ethanol mixture as *P*-transmitting fluid (Angel *et al.*, 2007); the ruby fluorescence shift (Mao *et al.*, 1986) and the quartz equation of state (Angel *et al.*, 1997) were used for the pressure measurement. The *in-situ* low temperature experiments (Gatta *et al.*, 2012, 2013a, 2013b) were performed, down to approximately 110 K, using an Oxford Diffraction Gemini single-crystal diffractometer (Mo-*K*α radiation) equipped with a CCD detector and a nitrogen gas-flow cryostat. The high-temperature behavior of cancrinite (Gatta *et al.*, 2014) was also studied, up to 823 K, using a Phillips PW1100 point-detector single-crystal diffractometer equipped with a microfurnace.

THERMOELASTIC BEHAVIOR

The experimental *V-P* data were fitted to II-order or III-order Birch-Murnaghan equations of state (BM-EoS; Angel, 2000), while "linearized" BM-EoS (Angel, 2000) were used to model the axial *P*-behavior (Table 1). The low-temperature (*i.e.*, *T* ≤ 293 K) data were fitted to the following equation: $x(T) = x_{Tr}\cdot\exp[\alpha_x\cdot(T-Tr)]$, where *x* is a unit-cell parameter (*V*, *a*, *c*), *T*r the lowest experimental temperature and α_x the thermal expansion coefficient of the unit-cell parameter *x*, which was fixed to be constant due to the low number of experimental data and the limited *T*-range (Table 2). The studied davyne-subgroup minerals (*i.e.*, davyne *sensu stricto* and balliranoite) showed very similar elastic behaviors at high pressure and low temperature. The description of the high-pressure

elastic behavior of cancrinite and vishnevite is less trivial. In cancrinite, a slight increase in compressibility is shown at $P \geq 5.00(2)$ GPa, whereas in vishnevite an anomalously strong increase in compressibility is observed at $P \geq 3.43(4)$ GPa, suggesting a metastable high-P structural re-arrangement. Although all the studied minerals share a similar bulk compressibility at the low-P regimes, a significant difference in the elastic anisotropy is observed between the members belonging to the two subgroups: the [0001] direction is always the most compressible/expandable one, but the anisotropic scheme is more pronounced in cancrinite and vishnevite (Tables 1, 2).

Table 1 - Isothermal (293 K) elastic parameters of cancrinite, vishnevite, balliranoite and davyne.

Isothermal elastic parameters								
Unit-cell volume								
	P-range (GPa)	**V_0 (Å³)**	**K_{V0} (GPa)**	**K_V'**	**P-range (GPa)**	**V_0 (Å³)**	**K_{V0} (GPa)**	**K_V'**
Cancrinite	0.0001-4.62	703.3(7)	45(2)	6(1)	5.00-6.63	715(4)	40(2)	4
Vishnevite	0.20-2.47	733.8(8)	49(4)	5.4(33)	3.83-7.40	757(6)	30(3)	2.6(5)
Balliranoite	0.0001-6.77	735(1)	48(3)	4.0(10)				
Davyne	0.38-7.18	761.6(5)	46.5(11)	3.7(3)				
Unit-cell linear parameters: a								
	P-range (GPa)	**a_0 (Å)**	**K_{a0} (GPa)**	**K_a'**	**P-range (GPa)**	**a_0 (Å)**	**K_{a0} (GPa)**	**K_a'**
Cancrinite	0.0001-4.62	12.603(7)	52(6)	11(4)	5.00-6.63	12.63(2)	58(4)	4
Vishnevite	0.20-2.47	12.765(3)	56(4)	7.3(32)	3.83-7.40	12.844(19)	40(3)	1.8(4)
Balliranoite	0.0001-6.77	12.654(6)	54(4)	4.6(14)				
Davyne	0.38-7.18	12.814(2)	50.3(9)	4.0(3)				
Unit-cell linear parameters: c								
	P-range (GPa)	**c_0 (Å)**	**K_{c0} (GPa)**	**K_c'**	**P-range (GPa)**	**c_0 (Å)**	**K_{c0} (GPa)**	**K_c'**
Cancrinite	0.0001-4.62	5.115(3)	34(2)	2.8(8)	5.00-6.63	5.196(16)	20.6(14)	4
Vishnevite	0.20-2.47	5.202(2)	37(2)	5.0(20)	3.83-7.40	5.33(3)	16(3)	3.6(5)
Balliranoite	0.0001-6.77	5.305(2)	40(2)	3.3(6)				
Davyne	0.38-7.18	5.3561(9)	40.3(7)	3.2(2)				

Table 2 - Thermoelastic parameters at constant pressure (0.0001 GPa) of cancrinite, vishnevite, balliranoite and davyne.

Thermo-elastic parameters at 0.0001 GPa						
Unit-cell volume						
	T-range (K)	**V_0 (Å³)**	**α_V (10⁻⁵ K⁻¹)**	**T-range (K)**	**V_0 (Å³)**	**$\alpha_{V(303K,1bar)}$* (10⁻⁵ K⁻¹)**
Cancrinite	100-293	698.2(6)	3.8(7)	303-748 748-823	707.50(5) 705.5(10)	4.88(8) 3.1(6)
Balliranoite	108-293	732.7(3)	4.6(4)			
Davyne	110-293	751.0(3)	4.2(4)			
Unit-cell linear parameters: a						
	T-range (K)	**a_0 (Å³)**	**α_a (10⁻⁵ K⁻¹)**	**T-range (K)**	**a_0 (Å³)**	**$\alpha_{a(303K,1bar)}$* (10⁻⁵ K⁻¹)**
Cancrinite	100-293	12.580(3)	0.7(2)	303-748 748-823	12.6237(3) 12.618(9)	1.16(3) 0.6(3)
Balliranoite	108-293	12.636(3)	1.4(2)			
Davyne	110-293	12.754(2)	1.4(1)			
Unit-cell linear parameters: c						
	T-range (K)	**c_0 (Å³)**	**α_c (10⁻⁵ K⁻¹)**	**T-range (K)**	**c_0 (Å³)**	**$\alpha_{c(303K,1bar)}$* (10⁻⁵ K⁻¹)**
Cancrinite	100-293	5.096(2)	2.1(3)	303-748 748-823	5.1264(3) 5.116(6)	2.58(8) 1.9(5)
Balliranoite	108-293	5.300(1)	1.7(2)			
Davyne	110-293	5.3300(7)	1.6(1)			
* Refined from the Berman (1988) equation of state						

STUCTURE DEFORMATION MECHANISMS AND ROLE OF THE EXTRAFRAMEWORK POPULATION

The *T*- and *P*-induced structure evolution of the studied cancrinite-group minerals is mainly governed by the tilting of the rigid (Si, Al)O$_4$ tetrahedra about the shared oxygen hinges. An inspection of the Si-O-Al intertetrahedral angles *versus* temperature or pressure shows that two clearly different trends can be defined for the cancrinite- and davyne-subgroup minerals, respectively. In the first subgroup, all the four symmetry-independent Si-O-Al angles vary with *T* or *P*. In the second subgroup, no significant variations of the Si-O2-Al angle are observed and the Si-O1-Al angle always shows the strongest change with *T* or *P* (Fig. 2).
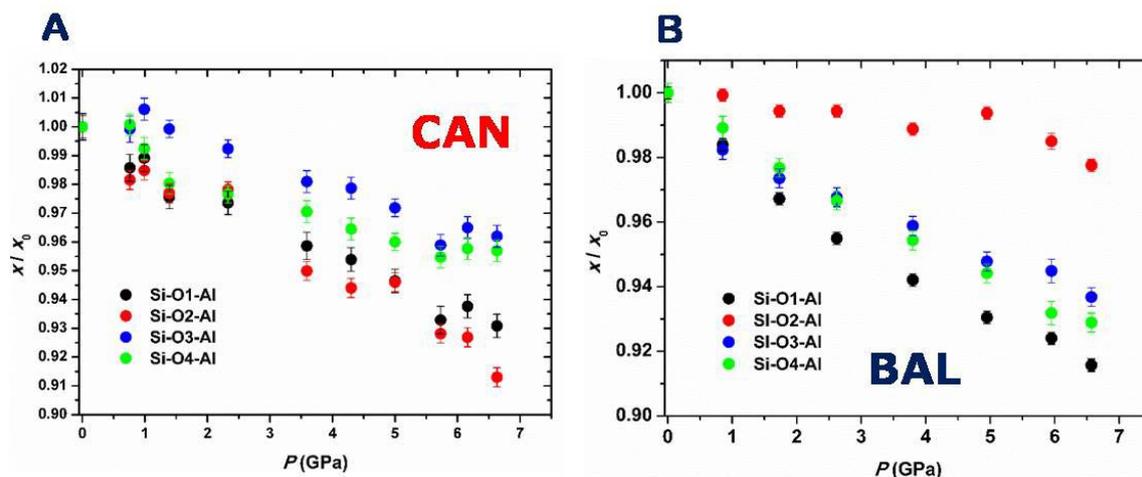

Fig. 2 - *P*-induced evolution of the Si-O-Al intertetrahedral angles in cancrinite (A) and balliranoite (B).

These different trends, likely governed by the different coordination environments of the cations filling the cages (*i.e.*, Na$^+$ or Ca^{2+}), are the basis of different deformation mechanisms between the two subgroups. The framework deformation along the [0001] crystallographic direction is controlled by the tilting of the tetrahedra forming the *dzc* chains, around the O3 and O4 hinges, which is reflected by the Si-O3-Al and Si-O4-Al intertetrahedral angles (Fig. 1). The behavior of these angles does not show significant differences between the two subgroups of minerals (Fig. 2) and the same deformation mechanism (*i.e.*, compression/expansion of the *dzc* chains) is observed. The main differences between the two subgroups are shown by the mechanisms accommodating the strain within the (0001) plane, mainly governed by the tilting of the tetrahedra around the O1 and O2 hinges (Fig. 1), as reflected by the Si-O1-Al and Si-O2-Al intertetrahedral angles (Fig. 2): 1) In cancrinite-subgroup minerals, the 6-membered rings (corresponding to the cage-bases) deform in response to (*P*, *T*)-gradients with a significant ditrigonal rotation, which is less pronounced in davyne-subgroup minerals; 2) The *can* units (cages, Fig. 1) also show different (*P,T*)-induced deformations within the two subgroups: *i*) in cancrinite and vishnevite, cages undergo a significant "flattening" with increasing *P* or decreasing *T; ii*) in davyne and balliranoite, the shortening along the O2-O2 (Fig. 1) diameter leads to a "compression" within the (0001) plane of the same magnitude as the compression along [0001], resulting in a "homogeneous shrinking" of the cages.

The characterization of the potential role played by the channel extraframework population on the structure evolution at non-ambient conditions is less linear: 1) in cancrinite, davyne and balliranoite, the channel population does not undergo any relevant change of its configuration at high-pressure or low-temperature; 2) on the contrary, in vishnevite a significant re-arrangement of the channel population takes place at H*P*: *i*) at *P* ≤ 3.24(2) GPa, the SO$_4$ tetrahedron (lying at the center of the channel, Fig. 1) shows both "upward" and "downward" configurations; *ii*) at *P* ≥ 3.43(2) GPa, a unique new configuration, with ~ 60° rotation around [0001] of the three oxygen atoms of the basis, occurs (simulating the configuration of the planar CO$_3$ group in

cancrinite). This re-arrangement of the SO_4 tetrahedron promotes the migration of the K (at $M1$) and Na (at $M2$) cations toward the center of the channel.

HIGH-TEMPERATURE BEHAVIOR OF CANCRINITE

The main results from the study on the high-temperature behavior of cancrinite can be summarized as follow: 1) the unit-cell volume evolution with temperature shows a continuous trend up to 748 K ("hydrous expansion regime"). The thermo-elastic parameters refined within this *T*-range (303-748 K) are reported in Table 2; 2) at 748 K, a slow dehydration process takes place, maintaining the same anisotropic scheme, being the compression along *c* higher than that along *a*; 3) when the dehydration process is completed, a (quasi)-anhydrous structure was refined and a unit-cell expansion is shown up to 823 K, where the broadening of the diffraction peaks suggests an incoming structural collapse.

CONCLUSIONS

All the studied cancrinite-group minerals show a similar *V*-compressibility and -expansivity at ambient conditions, but the cancrinite- and davyne-subgroup minerals, respectively, show a different thermo-elastic anisotropic scheme, which is related to different structure deformation mechanisms likely governed by the different cage population. At least in vishnevite, also the channel population was found to influence significantly the elastic and structural behavior at high pressure. These results suggest the relevance of modeling the interplay between the framework topology and the extraframework population, not only for cancrinite-group minerals, but for all the open-framework materials. The structure stability of the cancrinite-group minerals at high pressure is impressive if we consider their microporous nature. The experimental findings of this study provide the first thermoelastic parameters of the CAN-group minerals, which can be used to model the phase stability of this class of minerals with their petrological and industrial implications.

REFERENCES

Angel, R.J. (2000): Equations of state. *In*: "High-Temperature and High-Pressure Crystal Chemistry", R.M. Hazen & R.T. Downs, eds. *Rev. Mineral. Geochem.*, **41**, 35-60.

Angel, R.J., Allan, D.R., Miletich, R., Finger, L.W. (1997): The use of quartz as internal pressure calibrant in high-pressure crystallography. *J. Appl. Crystallogr.*, **30**, 461-466.

Angel, R.J., Bujak, M., Zhao, J., Gatta, G.D., Jacobsen, S.J. (2007): Effective hydrostatic limits of pressure media for high-pressure crystallographic studies. *J. Appl. Crystallogr.*, **40**, 26-32.

Baerlocher, C., McCusker, L.B., Olson, D.H. (2007): Atlas of zeolite framework types, 6th ed. Elsevier, Amsterdam, 398 p.

Bao, Y., Grutzeck, M.W., Jantzen, C.M. (2005): Preparation and properties of hydroceramic waste forms made with simulated Hanford low-activity waste. *J. Am. Ceram. Soc.*, **88**, 3287-3302.

Berman, R.G. (1988): Internally-consistent thermodynamic data for minerals in the system $Na_2O-K_2O-CaO-MgO-FeO-Fe_2O_3-Al_2O_3-SiO_2-TiO_2-H_2O-CO_2$. *J. Petrol.*, **29**, 445-522.

Bonaccorsi, E. & Merlino, S. (2005): Modular microporous minerals: Cancrinite-davyne group and C-S-H phases. *In*: "Micro- and mesoporous mineral phases", G. Ferraris & S. Merlino, eds. *Rev. Mineral. Geochem.*, **57**, 241-290.

Deer, W.A., Howie, R.S., Wise, W.S., Zussman, J. (2004): Rock-forming minerals. Framework silicates: silica minerals, feldspathoids and the zeolites (Vol. 4B). The Geological Society, London, 982 p.

Gatta, G.D., Lotti, P., Kahlenberg, V., Haefeker, U. (2012): The low-temperature behaviour of cancrinite: an *in situ* single-crystal X-ray diffraction study. *Mineral. Mag.*, **76**, 933-948.

Gatta, G.D., Lotti, P., Kahlenberg, V. (2013a): The low-temperature behavior of balliranoite (CAN topology): an in-situ single-crystal X-ray diffraction study. *Micropor. Mesopor. Mat.*, **174**, 44-53.

Gatta, G.D., Lotti, P., Nénert, G., Kahlenberg, V. (2013b): On the crystal structure and low-temperature behaviour of davyne: a single-crystal X-ray and neutron diffraction study. *Micropor. Mesopor. Mat.*, **185**, 137-148.

Gatta, G.D., Comboni, D., Alvaro, M., Lotti, P., Cámara, F., Domeneghetti, M.C. (2014): Thermoelastic behavior and dehydration process of cancrinite. *Phys. Chem. Minerals*, **41**, 373-386.

Lotti, P., Gatta, G.D., Rotiroti, N., Cámara, F. (2012): High-pressure study of a natural cancrinite. *Am. Mineral.*, **97**, 872-882.

Lotti, P., Gatta, G.D., Rotiroti, N., Cámara, F., Harlow, G.E. (2014a): The high-pressure behavior of balliranoite: a cancrinite-group mineral. *Z. Kristallogr.*, **229**, 63-76.

Lotti, P., Gatta, G.D., Merlini, M., Hanfland, M., (2014b): High-pressure behavior of davyne [CAN-topology]: an *in-situ* single-crystal synchrotron diffraction study, *Micropor. Mesopor. Mat.*, submitted.

Mao, H.K., Xu, J., Bell, P.M. (1986): Calibration of the ruby gauge to 800 kbar under quasihydrostatic conditions. *J. Geophys. Res.*, **91**, 4673-4676.

Pekov, I.V., Olysych, L.V., Chukanov, N.V., Zubkova, N.V., Pushcharovsky, D.Y. (2011): Crystal chemistry of cancrinite-group minerals with an AB type framework: a review and new data. I. Chemical and structural variations. *Can. Mineral.*, **49**, 1129-1150.

Zhao, H., Deng, Y., Harsh, J.B., Flury, M., Boyle, J.S. (2004): Alteration of kaolinite to cancrinite and sodalite by simulated Hanford tanks waste and its impact on cesium retention. *Clays Clay Miner.*, **52**, 1-13.